

# Simulation of rotating detonation engine by OpenFOAM

Thien Xuan Dinh<sup>\*†</sup>, Masatake Yoshida<sup>\*</sup>, and Shuichi Ishikura<sup>\*</sup>

<sup>\*</sup>Computational Science Division, Explosion Research Institute Inc.,  
3F, Dai 2 Tanaka Building, 3-5-2 Hongo, Bunkyo-ku, Tokyo, 113-0033 JAPAN  
Phone: +81-3-6803-2263

<sup>†</sup>Corresponding author: thien@bakuhatu.jp

Received: June 1, 2018 Accepted: January 25, 2019

## Abstract

This reports the primitive simulation of rotating detonation engine (RDE) using an OpenFOAM code developed by the Explosion Research Institute Inc. (ERI). To be able for such simulations, the code possesses the ability to cover the whole speed spectrum of deflagration-to-detonation (DDT) transition and the adaptive mesh refinement to capture detonation front. The code was firstly validated to the simulation of DDT in a tube with obstacles. It showed that the code reproduces well the flame throughout DDT in comparison with experiment. Secondly, the code was used to simulate the detonation wave in a simple RDE. With the code, we can adjust the condition that allows creating the detonation wave move around the chamber. This is very promised for the simulation of RDE in engineering.

**Keywords:** rotating detonation engine, deflagration-to-detonation transition, hybrid PISO-KT, adaptive mesh refinement, OpenFOAM

## 1. Introduction

A RDE contains a detonation wave that propagates continuously around an annular combustion chamber while the fuel was supplied to one end of the chamber<sup>1</sup>. Therefore, simulation of RDE poses the serious problems since it relates to detonation. Detonation requires a scheme that is capable to capture shock wave as well as a fine mesh for the chemical reaction<sup>2</sup>. This limits the simulation in very tiny RDE whose scale of millimeter. Instead of using uniform mesh, we try to reproduce accurately the energy release from the chemical reaction which is the dominant factor to accelerate the flame front by using adaptive mesh refinement (AMR)<sup>3</sup>. This method refines mesh around the flame front and coarsening mesh size in the others. This reduces greatly mesh grid number in comparison with using uniform mesh.

Furthermore, from the ignition, the flame in RDE accelerates from deflagration at low speed of order meter per second to detonation at high speed of kilometer per second, i.e. DDT<sup>4</sup>. The separation of speed regime in DDT requires a special treatment in numerical simulation. Usually, a numerical method is designated for either low or high-speed regimes separately. This requires the user

to manually switches solver appropriately while performing RDE simulation between two solvers: one for low speed flow and one for high speed flow. Alternatively, the hybrid schemes can switch between low speed scheme and high speed scheme dynamically dependent on the local flow speed. Among the hybrid schemes, the hybrid<sup>5</sup> of Pressure-Implicit with Spitting of Operator (PISO) and Kurganov-Tadmor (KT) is a promised method because these schemes are simple to implement in a code.

Although the AMR method is used, the massive computation for simulation of RDE is unavoidable because the flame front might have wide area where the several cell layers are necessary to refine. As a solution, we use OpenFOAM<sup>6</sup>, an open source code mainly for computational fluid dynamics. The free license feature of OpenFOAM allows user using many processors in their massive computation. Furthermore, with OpenFOAM, we can customize a solver fitting to the needs for simulation of DDT.

In this paper, we presented the development of the solver including a hybrid PISO-KT and AMR ability based on OpenFOAM. The solver is verified with the experiment data and applied to reproduce the detonation

wave in a simple RDE. The following of the paper structure is: first, the governing equations was briefly described; then the simulation of DDT in a rectangular tube with obstacle and detonation wave in a simple RDE and results were presented; finally, conclusion remark was discussed.

## 2. Numerical method

### 2.1 Governing equations

The fully coupled gas governing equation and the detail chemical reactions can be written as<sup>7)</sup>

$$\frac{\partial \rho}{\partial t} + \nabla \cdot (\rho U) = 0 \quad (1)$$

$$\frac{\partial \rho U}{\partial t} + \nabla \cdot (\rho U U) = -\nabla p + \nabla \cdot \sigma \quad (2)$$

$$\frac{\partial \rho E}{\partial t} + \nabla \cdot (\rho U E) = -\nabla \cdot (\sigma \cdot U + q) - \frac{dp}{dt} - Q \quad (3)$$

$$\frac{\partial \rho Y_k}{\partial t} + \nabla \cdot (\rho U Y_k) = R_k \quad (4)$$

Here  $U$  is velocity,  $\rho$  is the density,  $p$  is pressure,  $E$  is the total energy,  $\sigma$  is the viscous stress tensor,  $q$  is the diffusive heat, and  $Y_k$  is the mass fraction of  $k^{\text{th}}$  specie. The notation  $Q$  and  $R_k$  are the heat and mass source from the reaction whose forward and reverse reaction rates are calculated by Arrhenius law. The gas is considered as perfect gas.

### 2.2 Hybrid PISO-KT scheme

The above governing equations are solved iteratively by Finite Volume Method, using OpenFOAM platform. In the standard PISO<sup>8)</sup>, the predictor velocity is written as  $U = H(U)/A - \nabla \cdot p/A$ , then by replacing this into Equation (1) we have

$$\frac{\partial \rho}{\partial t} + \nabla \cdot \left[ \rho \frac{H(U)}{A} \right] - \nabla \cdot \left[ \rho \frac{\nabla p}{A} \right] = 0 \quad (5)$$

The mass flux  $\dot{m} = \nabla \cdot (\rho H(U)/A) - \nabla \cdot (\rho \nabla p/A)$  in Equation (5) is rewritten as the summation of left and right mass flux as  $\dot{m} = \dot{m}_+ + \dot{m}_-$ . The left and right mass fluxes are  $\dot{m}_+ = \alpha_+ \rho_+ \phi_+$  and  $\dot{m}_- = \alpha_- \rho_- \phi_-$ , where  $\rho_{\pm}$  and  $\phi_{\pm}$  are the density and volume flux on the left and right of a cell face. The coefficients  $\alpha_{\pm}$  are simply obtained by KT<sup>9)</sup>. The convection terms of the governing equations are then explicitly computed as, where  $\phi$  can be 1, velocity, energy, specie mass fraction

$$\nabla \cdot (\rho U \phi) = \chi \dot{m}_+ \phi_+ + [(1 - \chi) \dot{m}_+ + \dot{m}_-] \phi_- \quad (6)$$

The bending coefficient  $\chi$  is between 0 and 1. The coefficient  $\chi$  is dynamically determined by the Mach number,  $M_f$ , and Courant–Friedrich–Levy,  $CFL_f$ , number at the cell face as

$$\chi = \min \left( \frac{M_f}{CFL_f}, 1 \right) \quad (7)$$

### 2.3 Adaptive mesh refinement

In the current method, the refined cell is divided into 8 cells since its each direction is split into two equal layers. Therefore, the refined mesh cells will be split into  $8^n$  cells

where  $n$  is level of split determined by user if the considered parameter in that cell meets the defined criterion.

For DDT simulation one criterion for AMR is the flame position. Accurate capturing flame front is crucial in evaluating flame acceleration. In the direct reaction, the flame position will be the location where the reaction occurs or the reaction heat  $Q$  of Equation. 3 differs from zero. For facilitation setting criterion, the normalization was used thus the first criterion is

$$\frac{|Q|}{\max(|Q|)} \geq \varepsilon_1 \quad (8)$$

Additionally, the mesh is refined where the normalized gradient of velocity is greater than a designed threshold as

$$\frac{|\nabla U|}{\max(|\nabla U|)} \geq \varepsilon_2 \quad (9)$$

In our solver, these two criteria is combined into single boolean criterion as

$$\frac{|Q|}{\max(|Q|)} \geq \varepsilon_1 \text{ and } \frac{|\nabla U|}{\max(|\nabla U|)} \geq \varepsilon_2 \quad (10)$$

where  $\varepsilon_1$  and  $\varepsilon_2$  are the input by user.

## 3. Simulation and results

### 3.1 DDT in a tube

The DDT in centimeter scaled rectangular tube as shown in Figure 1 was simulated by the solver. The tube is filled with premixed hydrogen–air at stoichiometric ratio. The initial temperature and pressure are 298.15K and 0.1 MPa. The flame was ignited at the center of the left wall. The tube has the length of 2m. The contraction located at the distance of 0.96m from the ignition point. In the contraction section, there are 6 obstacles whose dimension is  $1.5 \times 1.5 \text{ cm}^2$ . The obstacles are located eventually with the interval of 30cm. The first obstacle is 43.2cm away from the contraction.

The tube was discretized in to mesh grid system with the typical cell size of 3.75mm, which is referred as the base mesh. The mesh around flame front and high velocity gradient regions are refined up to 2 levels. All the simulations were carried out on a single CPU, and they took approximately 72 hours of wall clock.

The simulation results are shown in Figure 2. Figure 2 (a) depicts a snapshot of the mesh refinement with the move of the flame front. In this case, the AMR was performed per 10 computational time steps. This does not impair the simulation results since the flame takes almost 10 computational steps to go beyond the refined mesh region.

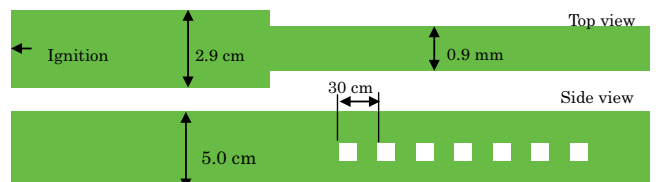
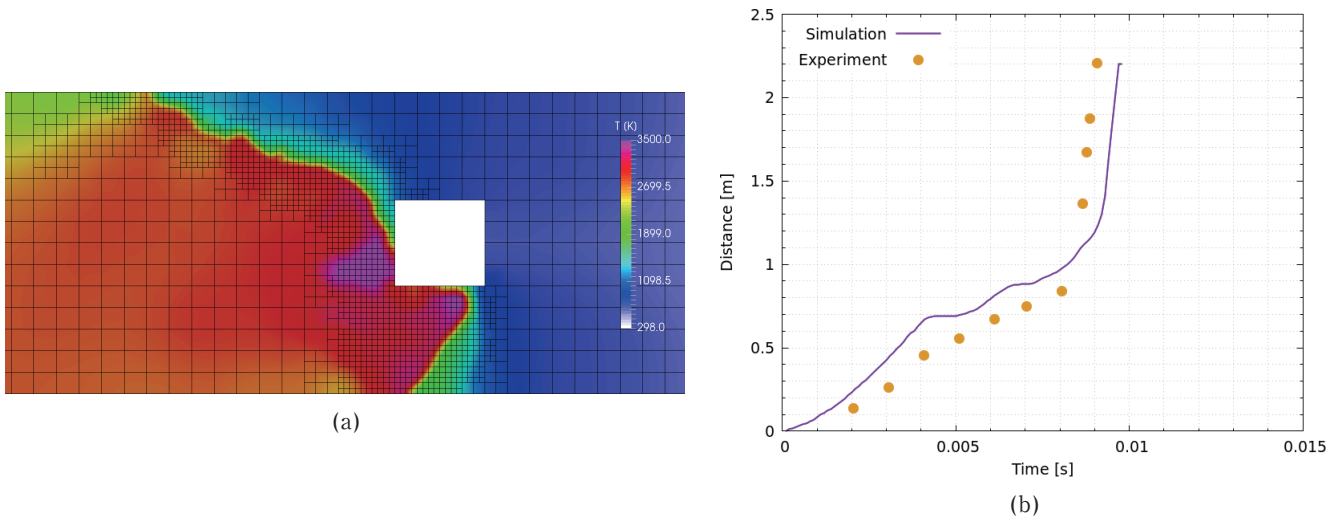


Figure 1 The sketch of the experiment tube.



**Figure 2** (a) The flame at the detonation occurrence. (b) The variation of flame position with time.

The propagation of flame in comparison with experiment data is shown in Figure 2(b). The time-dependent flame position quite differs from the experiment counterpart in the deflagration region. Before 0.005s, the simulation flame travels faster than experiment data. However, after this time, the flame slows down and has velocity compatible to experimental counterpart. Like the experiment, the simulation flame turns to detonation at around 0.009 s. The simulation detonation velocity is well agreed with that of the experiment as the slope of the simulation time-distance profile is similar to that of the experimental counterpart.

### 3.2 Detonation wave in a RDE

The considered RDE is shown in Figure 3. It is a hollow cylindrical tube with the outer diameter of 100mm and thickness of 5 mm. One quarter of the RDE is initially filled with air and the other three quarters are filled with fuel, a premixed hydrogen-air at stoichiometric ratio at standard temperature of 298 K and pressure of 0.1 MPa. The RDE is ignited at an edge of the fuel-air region. This aims to create the one directional detonation wave. While the detonation wave is traveling, the fuel is introducing to the RDE through the inlet at the speed so that when detonation wave completes 3/4 perimeter of the RDE, the fuel completes the path from the inlet to the outlet.

Figure 4 depicts the time revolution of the detonation wave the RDE. The figure shows that the detonation wave completes 3/4 perimeter in 0.12 ms, i.e. detonation speed is  $1970 \text{ m s}^{-1}$ . This is well agreed with the experiment detonation velocity of hydrogen-air mixture at stoichiometric ratio (ca.  $1980 \text{ m s}^{-1}$ ). It shows that the code is applicable to reproduce detonation wave in a typical large engineering RDE.

### 4. Conclusion

We have presented the simulation of simple RDE using our developed code based on OpenFOAM. The solver was verified with the DDT in a tube with obstacles in downstream. The simulation flame propagation was well agreed with the experimental data. The solver then was applied to simple RDE. The one-directional detonation

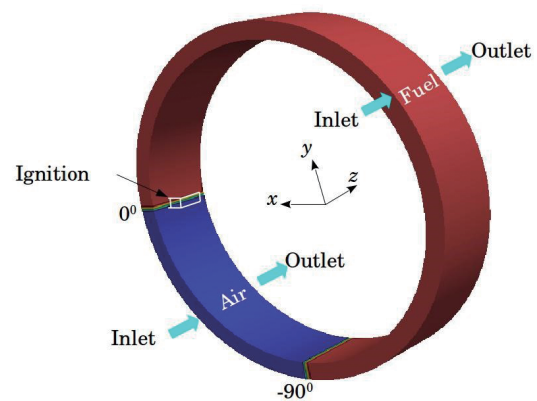


**Figure 3** The configuration of the rotating detonation engine.

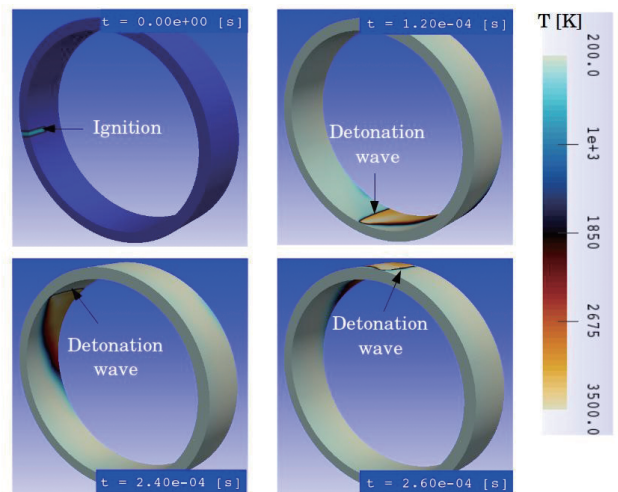


**Figure 4** The revolution of detonation wave.

wave was achieved in the combustion chamber. This attests that the solver promises a good simulation tool for the simulation of RDE engineering applications. A further test on engineering scale, i.e. meter, will be considered.

### References

- 1) S. M. Frolov, A. V. Dubrovskii, and V. S. Ivanov, Russian J. Phys. Chem. B, 7, 35–45 (2011).
- 2) C.M. Guirao, R. Knystautas, and J. H. Lee, NUREG/CR-4961 (1989).

- 3) M. Essadki, S. Chaisemartin, M. Massot, F. Laurent, A. Larat, and S. Jay, *Oil Gas Sci. Technol.*, 71 (2016).
- 4) G. Ciccarelli, J.L. Boccio, T. Ginsberg, C Finfrock, L. Gerlach, H. Tagawa, and A. Malliakos, *NUREG/CR-6509* (1998).
- 5) K. Matvey, B. Arina, and S. Sergei, *Proc. Com. Sci.*, Vol. 66, 43–52 (2015).
- 6) OpenFOAM Home Page. <https://openfoam.org/>(accessed: March 2017)
- 7) D. A. Bitter, *Comp. Syst. Eng.*, 4, 1–12 (1993).
- 8) R. I. Issa, *Mech. Eng. Report*, FS/82/15, Imperial College, London (1982).
- 9) C. J., Greenshields, H. G. Weller, L. Gasparini, and J. M. Reese, *Int. J. Num. Meth. Fluids*, DOI 10.1002/fld.2069 (2009).